Mon. Not. R. Astron. Soc. **000**, 000–000 (0000) Printed 14 January 2003 (MN LaTeX style file v1.4)

The topology and polarisation of sub-beams associated with the 'drifting' sub-pulse emission of pulsar B0943+10 — III. Analysis of Pushchino 103/40-MHz observations

Joanna M. Rankin[1,2], Svetlana A. Suleymanova[3] & Avinash A. Deshpande[4,5]
[1] *Sterrekundig 'Anton Pannekoek', University of Amsterdam, Netherlands NL-1098 : jrankin@astro.uva.nl*
[2] *On leave from: Physics Department, University of Vermont, Burlington, VT 05405 USA : rankin@physics.uvm.edu*
[3] *Pushchino Radio Astronomy Observatory, Lebedev Physical Institute, Moscow 117924, RUSSIA : suleym@prao.psn.ru*
[4] *Raman Research Institute, Bangalore 560 080 INDIA : desh@rri.res.in*
[5] *Current address: Arecibo Observatory, Box 53995, Arecibo, Puerto Rico 00612 : desh@naic.edu*

ABSTRACT
The rotating emission-beam system of pulsar B0943+10 has been explored in Paper I of this series using Arecibo observations at 430 and 111 MHz and in Paper II using Gauribidanur 35-MHz data. Here, we have the opportunity to study simultaneous, dual frequency observations, carried out at the Pushchino Radio Astronomy Observatory some 10 years ago at frequencies of 103 and 40 MHz. The apparent modulation periods (P_3) and circulation times derived from the eleven days of observations seem to fall into two distinct ranges, apparently correlated with profile-modal effects. The 103-MHz maps bear strong resemblance to the 111-MHz Arecibo sequence studied in Paper I, but show a variety of subbeam-intensity patterns; whereas, similar comments can be made about the 40-MHz maps in relation to the 35-MHz maps of Paper II. Most interesting here is the result that there is little correspondence between the subbeam maps at the two frequencies. Only for two of the observations do we find a correspondence between the pairs; one of the 'B'-mode sequences with an asymmetric pattern as well as a 'Q'-mode sequence occurring immediately prior to a transition to the 'B' mode. Finally, we find that our various 'B'-mode observations vary markedly in their profile linear polarisation. The strongest sequences suggest differing proportions of secondary-polarisation-mode power.

Key words: MHD — plasmas — pulsars: general, individual (B0943+10) — radiation mechanism: nonthermal — polarisation

I. INTRODUCTION

In this paper we continue our study of pulsar B0943+10's emission-beam pattern, making use of its remarkably stable 'drifting' subpulse sequences. While the potential of this situation was outlined in Deshpande & Rankin (1999),* Papers I and II of this series [Deshpande & Rankin (2001) and Asgekar & Deshpande (2001), respectively] have given detailed analyses of the star's subpulse modulation, using Arecibo observations at 430 and at 111.5 MHz and 35-MHz observations from the Gauribidanur Observatory.

These two programs of analysis have begun to reveal the character and dynamics of the pulsar's emission beam system. Observations separated by many years and over a broad frequency range have shown that its "B"-mode pulse sequences are produced by a pattern of just twenty subbeams which rotate counter-clockwise around the pulsar's 'nearer' magnetic axis in an interval of about 37 pulsar-rotation periods (P_1) or some 41 s. The striking circumstance that the pulsar's ('B'-mode) radiation consists of a vigesimal beam system over the full 35- to 430-MHz range of the observations strongly suggests that the radiation is produced within a system of emission columns, which, being 'seeded' in the acceleration region, rise up through the emission region and extend out well beyond it. A marked difference, however, between the 35-MHz observations and those at higher frequencies is that some individual subbeams (or a group of them) are more frequently weak or missing—though the vigesimal

* See also Deshpande (1999) and Rankin & Deshpande (1999)

Table I—Properties of the Observations

Date	ν (MHz)	mode	Good p#s	HRF p#s	MAP p#s	f_3(c/P_1)	$\hat{P}_3$ (P_1)	$<L>/<I>$ (%)
7.12.90	103	Q	34–280	25–280	153–280	—	36.5?	*28*
	40	Q	34–311	34–311	184–311	—	36.5?	*33*
	103	B	281–400	273–400	281–400	0.54817 ± 0.00069	36.485 ± 0.046	**39**
	40	B	312–400	312–400	312–400	0.5535 ± 0.0021	36.13 ± 0.13	39
8.12.90	103	B	145–400	145–400	145–400	0.53574 ± 0.00004	37.332 ± 0.003	**25**
	40		145–400	145–400	176–400	0.53587 ± 0.00059	37.322 ± 0.041	22
10.12.90	103	B	1–320	193–320	—	0.53108 ± 0.00008	37.659 ± 0.006	**46**
	40		1–400	1–400	—	0.53085 ± 0.00011	37.675 ± 0.008	38
16.12.90	103	B	2–400	142–397	—	0.54271 ± 0.00005	36.852 ± 0.003	**28**
	40		1–400	193–320	—	0.54520 ± 0.00020	36.684 ± 0.013	22
17.12.90	103	B	1–400	145–400	145–400	0.53015 ± 0.00003	37.660 ± 0.002	**37**
	40		1–100	1–128	1–100	0.53071 ± 0.00040	37.686 ± 0.028	31
20.12.90	103	Q	13–400	81–336	—	—	—	*28*
	40		13–400	81–336	—	—	—	*23*
22.12.90	103	Q	13–400	—	—	—	—	*26*
	40		13–400	—	—	—	—	*29*
23.12.90	103	B	60–340	81–336	81–336	0.53141 ± 0.00004	37.636 ± 0.003	**22**
	40		2–400	2–400	112–367	0.53058 ± 0.00012	37.695 ± 0.008	25
24.12.90	103	B	1–400	91–346	—	0.54238 ± 0.00003	36.875 ± 0.002	**22**
	40		1–400	1–400	—	0.54164 ± 0.00036	36.925 ± 0.025	30
26.12.90	103	B	60–340	91–346	91–346	0.54686 ± 0.00003	36.572 ± 0.002	**20**
	40		1–400	1–400	122–377	0.54738 ± 0.00010	36.538 ± 0.007	20
27.12.90	103	B	80–360	91–346	91–346	0.53234 ± 0.00003	37.570 ± 0.002	**25**
	40		1–400	1–400	122–377	0.53133 ± 0.00020	37.641 ± 0.014	30
28.12.90	103	Q	100–320	91–346	91–346	—	36.5?	*16*
	40		2–400	1–400	122–377	—	36.5?	*17*
11.02.91	103	Q	1–250	1–250	—	—	—	*26*
13.02.91	103	B	1–250	1–250	—	0.52788 ± 0.00003	37.887 ± 0.022	**40**
15.02.91	103	Q	1–250	1–250	—	—	—	*14*
23.01.92	103	B	2–400	81–336	—	0.53101 ± 0.00002	37.664 ± 0.014	**70**

Notes: a) The tabulated f_3 values refer to the interpolated centroids of the various spectral features (see text), and the error bars indicate the formal (1-σ) uncertainties in their estimation (and are thus not the feature widths). b) The $\hat{P}_3$ values are not independently determined, but are computed as $20/f_3$. c) The 103-MHz $<L>/<I>$ values in the last column appear bold and the Q-mode values in italics, respectively, in order to facilitate comparison.

nature of the overall system is still strongly maintained—raising immediate questions about how the low and high frequency patterns correspond.

Moreover, the star's 'Q'-mode behaviour stands in fascinating contrast to that of the 'B' mode: The regular subpulse modulation—evidenced by the 0.53 c/P_1 fluctuation feature—disappears. The subpulses appear disorganized and, while weaker overall, some are remarkably bright, indeed brighter than any usually seen in 'B'-mode sequences. The average profile assumes a different form, and the secondary polarisation mode (hereafter, SPM and also PPM) predominates throughout the profile. Underlying this disorganization, we found evidence in Paper I that the overall beam system continues to rotate in the 'Q' mode, at perhaps a slightly different rate, even though only one or two subbeams remain active.

Here, we have the opportunity to study simultaneous, dual frequency observations of pulsar 0943+10 for the first time. §II discusses the observations, §III our efforts to determine the primary modulation frequences of the 'B'-mode sequences, and §§IV & V present the subbeam maps of the 'B'- and 'Q'-mode observations, respectively. Then, in §§VI and VII we discuss their polarisation and briefly summarize the results and conclusions.

II. OBSERVATIONS

The observations were conducted at the Pushchino Radio Astronomy Observatory (PRAO) using the BSA (Bolshaya Synfaznaya Antenna) at 103.13 MHz and the East-West arm of the DKR-1000 cylindrical paraboloid cross telescope at 39.898 MHz.† Most of the observations were carried out on 22 nights during 1990 December, and the 11 simultaneous pulse-sequence (hereafter PS) pairs used in this analysis were chosen for their relatively good signal-to-noise ratio (hereafter S/N) in both bands.‡ One could not ask for a

† The two instruments are fully described in the Pushchino Observatory website:http: //www.prao.psn.ru

‡ Several of these sequences were analysed earlier in Suleymanova *et al* (1998), but no use could then be made of their simultaneous character.

more diverse set of observations for initial study: As summarized in Table I, the dual-band observations on December 8, 10, 16, 17, 23, 24, and 27 are 'B'-mode sequences, marked by the usual asymmetrical profiles; Dec. 26 is an unusual 'B'-mode sequence with a nearly symmetrical double profile at 103 MHz; Dec. 7 records a transition from the 'Q' to the 'B' mode; and Dec. 20, 22 and 28 are entirely 'Q'-mode sequences. Also, we had available four later 103-MHz PSs, two each in the 'B' and 'Q' modes.

The signals from these linearly polarised arrays were fed to radiometers with 64x20-kHz contiguous channels (BSA) and 32x5-kHz channels (DKR-1000) in order to measure the total intensity and its spectral variations across the passband. The dedispersed pulses were referred to the frequency of the first channel—that is, to 103.130 and 39.898 MHz (hereafter, 103 and 40 MHz). This choice of frequencies makes the sampled windows of the two bands adjacent in time, apart from the overall dispersion delay of 31 P_1.

By observing a partially linearly polarised pulsar signal at adjacent frequencies the rotation measure can be obtained, which for observing frequencies of 40 and 103 MHz, gives RM=15±1 rad/m^2. The Faraday-modulation period Δf is related to the frequency f by Δf=1.748×10$^{-5}f^3/RM$ (f in MHz). In that the total passband exceeded (and was a multiple of) the Faraday-modulation period at these frequencies, the total intensity of the dedispersed pulses provides a reasonable estimate of Stokes parameter I. The fractional linear polarisation and its associated position angle (hereafter PA) χ were then determined for each sample—using a technique developed at Pushchino (Suleymanova, Volodin & Shitov 1988)—from the Faraday-rotation-induced, quasi-sinusoidal intensity modulation across the passband. The time resolutions were 6.98 ms or 2.29 mP_1 at both frequencies. Most of the observations were comprised of 400 pulse periods, although only for some 280 of these was 0943+10 well within the BSA's beam at 103 MHz.

Each of the 103-MHz sequences is thus modulated by the gain of the BSA during transit of the source, limiting the usable sequence to 280 periods, as above. Within this interval, the effects of interstellar scintillation largely appear to be averaged out, suggesting that the 20-kHz channel bandwidth exceeds the decorrelation bandwidth at 103 MHz. We see a very different behaviour at 40 MHz. The gain profile of the DKR-1000 appears to be roughly constant over the 400-pulse observations; however, the pulsar intensity is highly corrugated within this interval. "Flares" of 50 pulses or so are common, and for this reason we can see from the outset that it will not be easy to find sequences which are completely comparable at the two frequencies.

III. 'B'-MODE CIRCULATION-TIME DETERMINATION

The initial stages of our analysis will be familiar to readers of Papers I and II. We have computed the usual longitude-resolved fluctuation (hereafter, 'LRF') spectra as well as harmonic-resolved fluctuation ('HRF') spectra for each 'B'-mode sequence, resolving questions of aliasing to show that the star's primary subpulse modulation frequency f_3 is some 0.53 c/P_1. Examples of these spectra can be found in figs. 1 & 4 of Paper I, where a detailed description of their computation and display will be found. The argument in Paper I went on to show, in a variety of ways, that this modulation was produced by a set of just 20 circulating subbeams, which then define a tertiary modulation period of $20/f_3$ or some 37 P_1. The PRAO observations provide no strong, independent confirmation ('sidebands' or low frequency features) of the vigesimal character of this tertiary modulation period. We have carefully examined each sequence for such features, but no fully developed and reliable signature was identified.[§] Nonetheless, the stability and 20-fold character of 0943+10's tertiary modulation have been so well established in our foregoing analyses—and the current observations are so clearly compatible with those examined earlier—that we can proceed here confidently.

These selfsame steps were followed in our analysis of the Pushchino observations, and some of the parameters and results comprise Table I. We first computed LRF spectra for each sequence in order both to examine its average profile (so as to establish its centre) and to assess its coherence and quality. Some examples of these are given in Figures 1, 4 & 2. Here, we see the distinct profiles characteristic of the 'B' mode at 103 and 40 MHz in Figure 1, the unusual 'B'-mode profiles in Figure 3, and the distinct 'Q'-mode profiles in Figure 4, to which we will return in a later section. We also see here again the remarkable regularity or 'coherence' of the aliased 0.46-c/P_1 feature associated with the star's 'drift'—even at 40 MHz, though generally with a reduced precision. We then computed HRF spectra—using overlapping ffts of length 256 wherever possible—for appropriate sections of each 'B'-mode observation and then interpolated between adjacent Fourier amplitudes to estimate the frequency of the feature and its errors. Examples of the HRF spectra are displayed in Figure 2. We see in Table I that 8 of the 11 dual-band observations are entirely 'B'-mode sequences and that the end of the first day (7/12) is as well, though its brevity has limited the precision of the values determined. The resulting feature frequencies are tabulated in the column headed f_3 and the circulation times in the one labeled $\hat{P}_3$; the errors for both reflect the narrowness of the HRF feature and represent about two standard deviations.

Several interesting results seem to follow from this table. First, feature frequencies and circulation times of two differ-

§ Two observations with asymmetric polar-map patterns, 23/12 at 40 MHz and 27/12 at 103 MHz (see figs. 5 & 6), might have been expected to produce such features, just as were found in Paper II. On closer inspection, however, neither map is fully asymmetric. Such instances reiterate how unusual, or fragile, are the conditions which retain features related to the tertiary modulation period. The smooth modulation seen in the 35-MHz observations of Paper II resulted in the detectable tertiary modulation feature in the spectrum. In the absence of such smooth variation of intensities across the subbeam sequences, the modulation power gets shared by several harmonics of the tertiary modulation frequency, reducing the possibility of detecting any of them clearly above the noise.

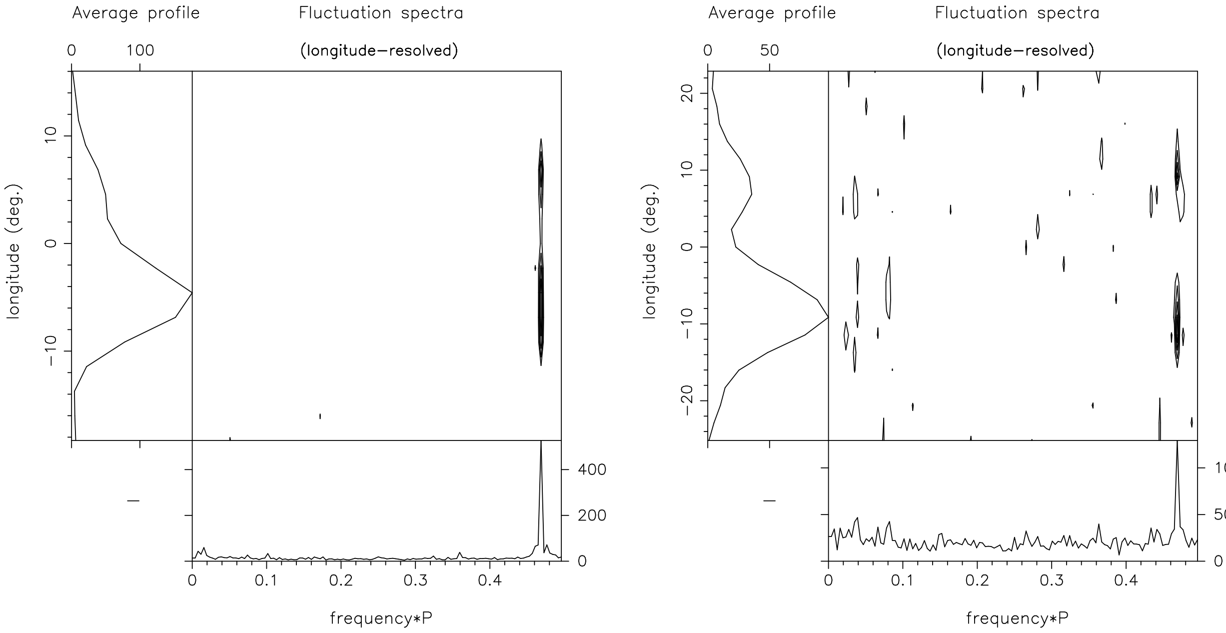

Figure 1. Characteristic 'B'-mode profiles and LRF spectra for pulsar B0943+10 on 23/12/90 at 103 (*left*) and 40 MHz (*right*). FFTs of length 256 were used. The body of the figures gives the amplitudes of the features as a set of contours. The average profiles (Stokes I) are plotted in the respective left-hand panels, and the integral spectra are given at the bottom of each figure. The pulse-sequence amplitudes were adjusted before analysis to remove any slow secular changes, so that any small $1/f$ 'tails' in the spectra have been suppressed.

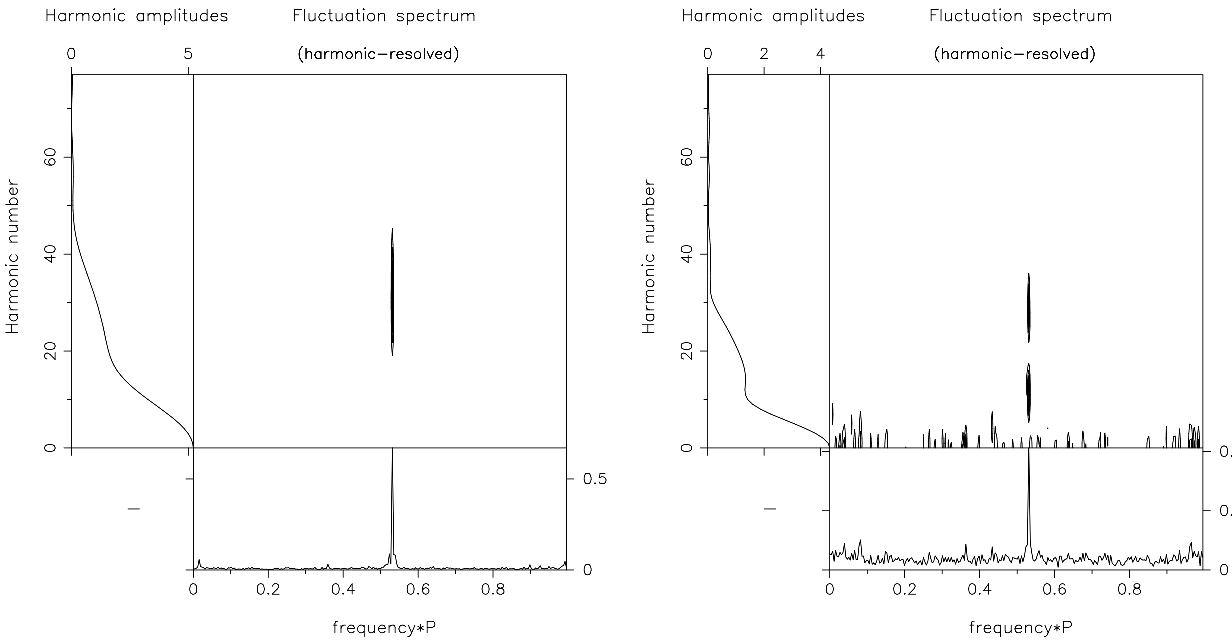

Figure 2. 'B'-mode HRF spectra for pulsar B0943+10 on 23/12/90 at 103 (*left*) and 40 MHz (*right*). These continuously sampled spectra resolve the aliasing of the pulsar's primary modulation feature, which we now see at about 0.54 c/P_1. Note also that the feature widths here are narrower, indeed barely resolved. See Paper I, fig. 4 for a complete description.

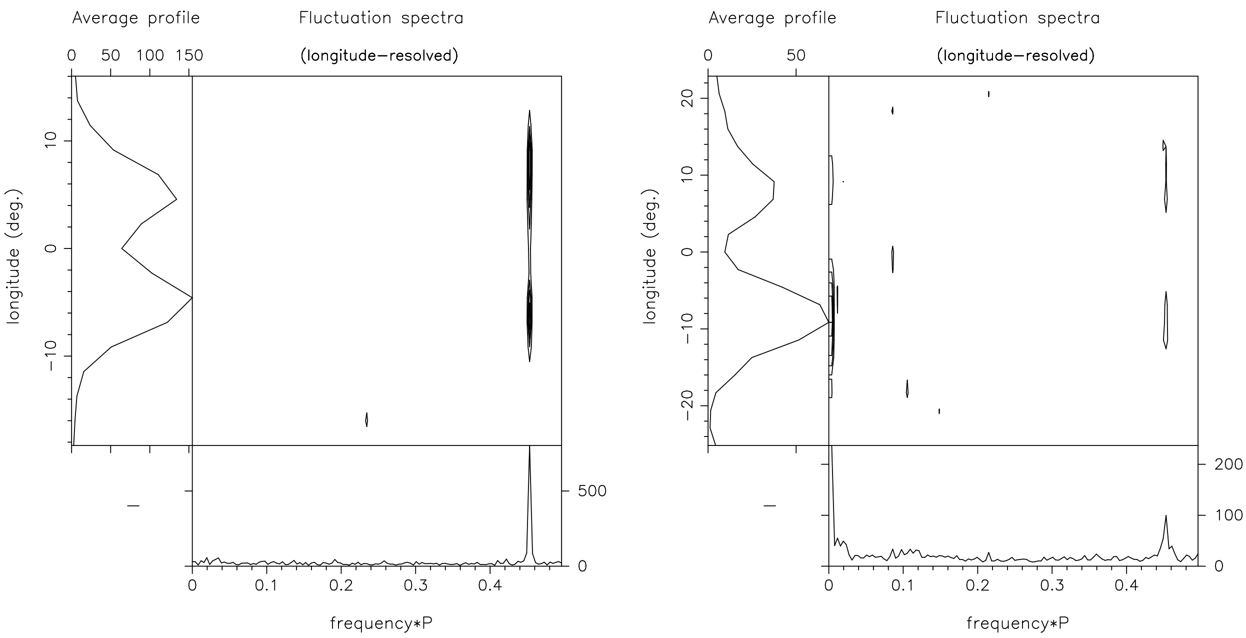

Figure 3. Unusual 'B'-mode profiles and LRF spectra on 26/12/90 at 103 (*left*) and 40 MHz (*right*) as in Fig. 1.

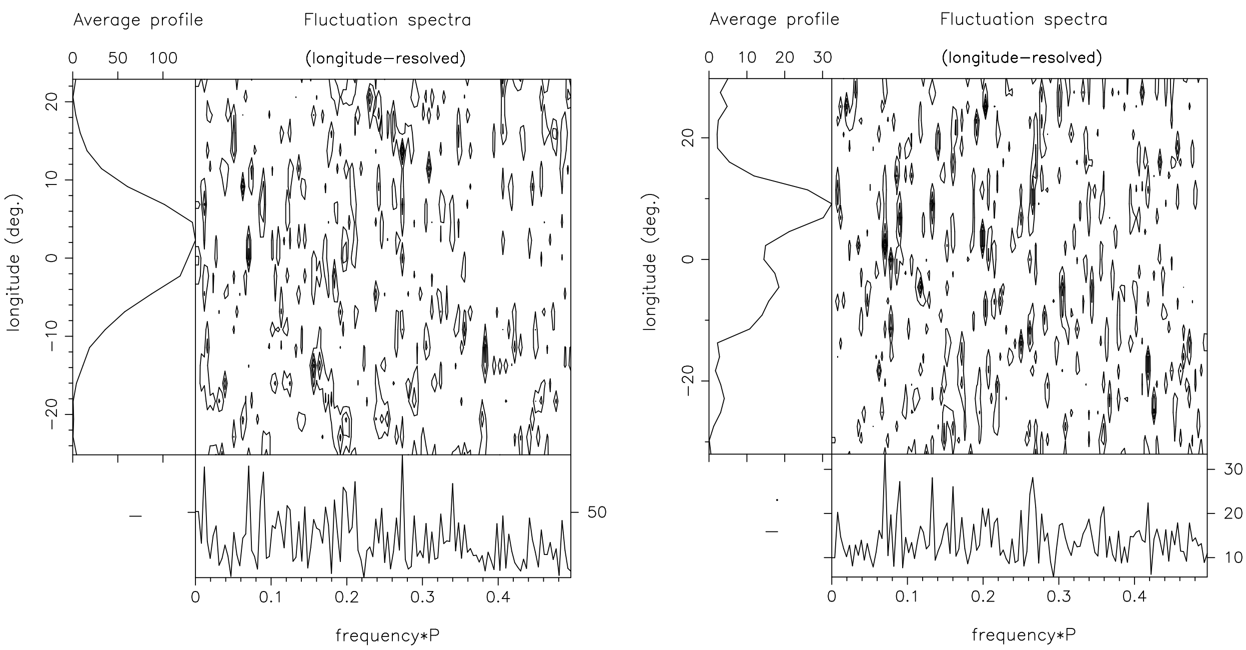

Figure 4. Characteristic 'Q'-mode profiles and LRF spectra on 28/12/90 at 103 (*left*) and 40 MHz (*right*) as in Fig. 1.

ent sorts occur among the observations: Most days exhibit f_3 values just over 0.53 c/P_1 and consequently $\hat{P}_3$ values well over 37 P_1 (with many near 37.7 P_1). However, other days have f_3 values over 0.54 c/P_1 and thus tertiary modulation periods under 37 periods—indeed, several around 36.5 P_1. It is notable that both the first sequence (7/12)—where the short 'B'-mode sequence immediately follows a transition from the 'Q' mode—and the fifth (26/12), whose unusual symmetric profile is reminiscent of 'Q'-mode forms, fall into this latter group. Further study yields the result that the $\hat{P}_3$ values correlate well with the profile forms: a) those observations with the usual 'B'-mode profiles, wherein the 103-MHz trailing component is much weaker (some 20%) than the leading (*cf.* the 103-MHz profiles in Figs. 2 & 2), all have $\hat{P}_3$s over 37 periods, whereas b) the other PSs with unusual 'B'-mode profiles (where the 103-MHz trailing component is 50% or more as intense as the leading one) all have $\hat{P}_3$s under 37 P_1. These unusual, more symmetrical 'B'-mode profiles are reminiscent of the symmetrical 'Q'-mode forms.

It is also worth noting that a range of f_3 values were found in Paper I (see Table 1), although they then did not fall into any discernible pattern. Now we can see that of the five observations, only the 430-MHz PS from 1972 has an f_3 value that corresponds to a $\hat{P}_3$ under 37 P_1, and here only just under. Nonetheless, we find that its profile [not shown here; see Backer *et al* (1975): fig. 4] is wider and more symmetric about the longitude of the magnetic axis than its 1992 counterpart.

The 'B'-mode sequences exhibit a highly 'coherent' modulation, and therefore the modulation frequencies and circulation times associated with some of them can be determined to a high precision. In reviewing them it is surprising to find that some of the respective 103- and 40-MHz observations pairs exhibit small modulation-frequency differences at a level of a few standard deviations. Moreover, these differences appear somewhat orderly: for the sequences with $\hat{P}_3 \geq 36.9 P_1$, the 40-MHz $\hat{P}_3$ value is equal to or a little longer than its 103-MHz counterpart; for those more 'Q'-like sequences with $\hat{P}_3$ values under 36.9 P_1, we find an apparent opposite behaviour. Of course, the numbers here are small, and sources of the errors uncertain—indeed, we might attribute a part of the differential to random changes in the average subbeam spacing—however, the ostensible order in the values bears further study as longer, higher quality PS pairs become available.

IV. MAPPING THE 103/40-MHZ 'B'-MODE BEAM STRUCTURE

With this preliminary analysis completed, we are now in a position to construct the subbeam maps using the 'cartographic' transformation discussed in Paper I [see eqs. (5–8)]. In addition to the circulation time $\hat{P}_3$ and the central longitude, this transformation requires as inputs a full specification of the observing geometry—entailing not only the usual magnetic latitude α and impact angle β—determined in Paper I to be 11.6° and -4.31°, respectively‖—but also our finding that the subbeam system rotates ccw around the 'emitting' magnetic axis, whereas the star revolves cw with respect to the 'nearer' rotation axis. Further, in order to ensure that our maps display the same pulses at the same positions for the two frequencies, we took the pulse number origin [k_0 in Paper I, eq.(6)] to be 31 larger at 40 MHz.

The 103-MHz subbeam maps divide into three different sorts: First, we have observations in which most of the 20 subbeams have roughly comparable intensities, the few others being weaker but not absent. This is apparently one of the usual 'B'-mode configurations, represented well by the 17 and 23/12 observations, and a polar map of the latter is given as an example in Figure 5 (*left*). Second, we see intervals in which several subbeams are much brighter than the others, dominating the pattern—though again, each of the 20 can be discerned. Examples of this kind occur on the 7, 8 and 26/12, and Figure 6 (*left*) shows this latter behaviour. Finally, we find observations in which the subbeam intensity is enhanced asymmetrically in one half of the pattern. Our 27/12 observation gives such an instance, which is shown in Figure 7 (*left*). Note that the presentation of the 103- and 40-MHz maps is slightly different: At 103 MHz, where the 'base' (*i.e.* azimuthal minimum) is well defined, we have subtracted it from the maps in the central panels before plotting; we found, however, that the 40-MHz maps were clearer without this 'base' removed.

In the first case—those PSs with rather little variation in their 103-MHz subbeam intensities—the corresponding 40-MHz maps bear little resemblance to their higher frequency counterparts. All three such days exhibit much more disordered, 'patchy' or asymmetric subbeam configurations with many subbeams hardly discernible—though the 20-fold character of the subbeam pattern is still very strongly maintained. The map of the 23/12 sequence in Figure 5 (*right*) exhibits both the disorderly character of the 40-MHz pattern and its strong asymmetry. Only the four subbeams at the top of the diagram and the two on the right are at all prominent; most others are much weaker and some are nearly absent. It is difficult to assess the correspondence between the 103- and 40-MHz patterns. The strong asymmetry in the lower frequency pattern is not at all apparent in the higher frequency one—at any orientation. Little more can be gleaned from the 17/12 sequence; the 40-MHz pattern is again asymmetric—as perhaps is the higher frequency one—but at different orientations. In any case, the usable portion of the 40-MHz sequence precedes that at 103 MHz, so they cannot be compared strictly (see Table I).

Very similar comments can be made for the pair of maps in Figure 6. Few, if any, of the several brightest beams at 103 MHz are particularly bright at 40 MHz, though the lower frequency pattern does show several particularly bright subbeams. Here we might describe the 40-MHz pattern as more 'patchy' than asymmetric. Two subbeams at 40 MHz dominate the pattern, and the corresponding beams at the higher frequency are not especially bright. Nearly identical comments can be made for the 8/12 patterns. The 7/12 one, however, though shorter, is interesting because it immediately follows a 'Q'-mode sequence. Here, both patterns are

‖ The results of Mitra & Rankin (2002) argue that we observe an outer cone in 0943+10, because inner cones seem to have virtually no radial increase at low frequency and thus cannot produce the evolution toward double profile forms seen there. An inner-traverse, outer cone model gives α and β values of some 15.4° and -5.69°, respectively. The cartographic transform, however, depends sensitively only on the ratio of these quantities—the PA sweep rate—so that maps using the inner- vs. outer-cone geometry will be virtually indistinguishable apart from their overall angular size. We have thus retained the inner-cone-model values here, so that the maps of all three papers can be compared directly.

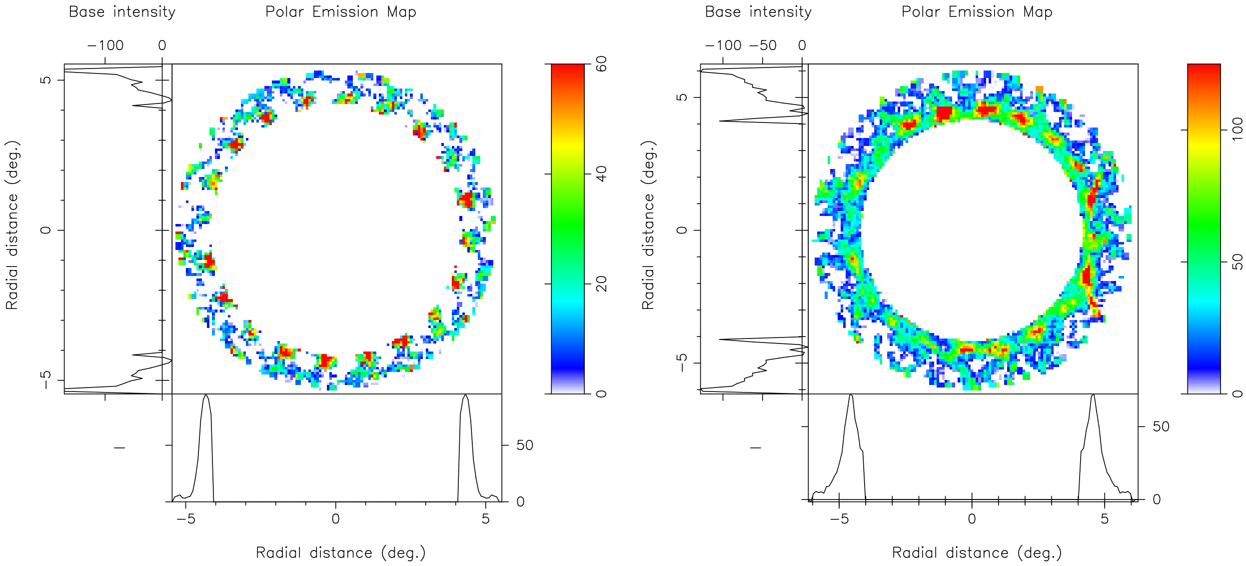

Figure 5. 'B'-mode polar maps for pulsar B0943+10 on 23/12/90 at 103 (*left*) and 40 MHz (*right*). These images reflect fully simultaneous sequences of 256 pulses. The polar map is projected onto the polar cap shown in the main panel, with the 'closer' rotational axis at the top of the diagram. The star rotates cw, causing the sightline to cut the ccw-rotating subbeam system from left to right. The bottom and the side panels show the average- and the 'base'-intensity profiles, respectively, as functions of the angular distance from the magnetic axis. The 103-MHz 'base' has been subtracted from the pattern in the central panel; whereas, the 40-MHz 'base' has not. The 103-MHz map is a good example of those in which most of the subbeams have roughly uniform intensity. Note the track of one unusually bright pulse at the right of the 40-MHz map.

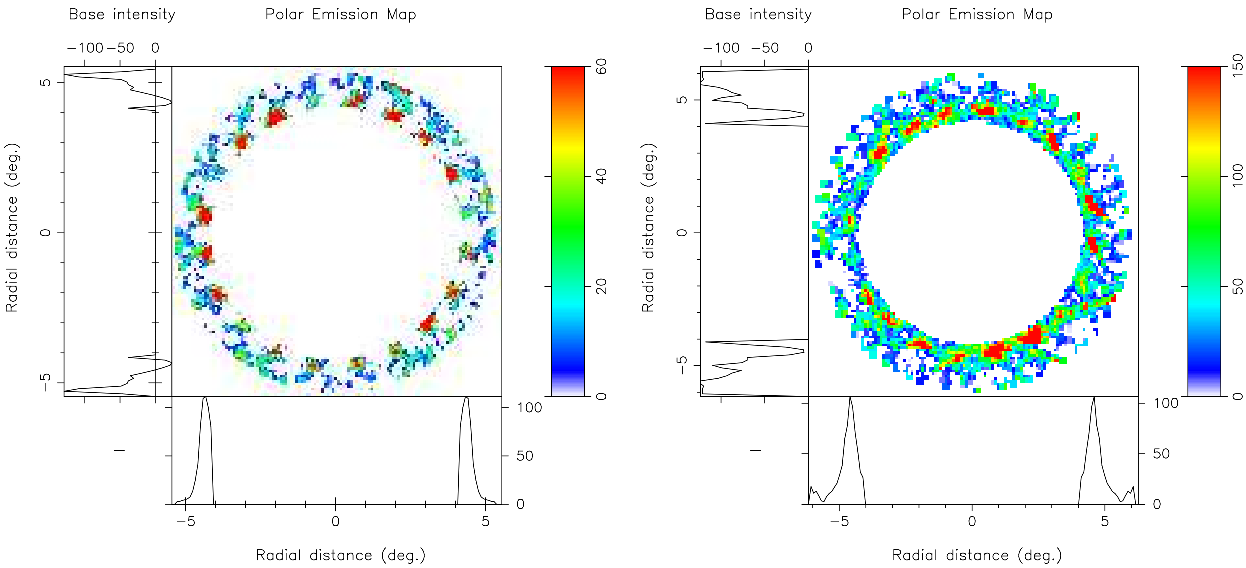

Figure 6. 'B'-mode polar maps on 26/12/90 at 103 (*left*) and 40 MHz (*right*) as in Fig. 5. This 103-MHz map is a good example of those in which a few subbeams tend to dominate the others.

dominated by a few bright subbeams, and little or no emission can be detected at the positions of others.

The somewhat asymmetric pattern in Figure 7 provides the most interesting apparent correspondence between the patterns at the two frequencies. The 103-MHz map exhibits a pattern with most of the bright subbeams at the top left of the map; whereas the 40-MHz pattern also has its brightest subbeams at the top left of the pattern (as well as a few weaker ones at the bottom). Indeed, a series of six bright subbeams at the upper left of both patterns are among the

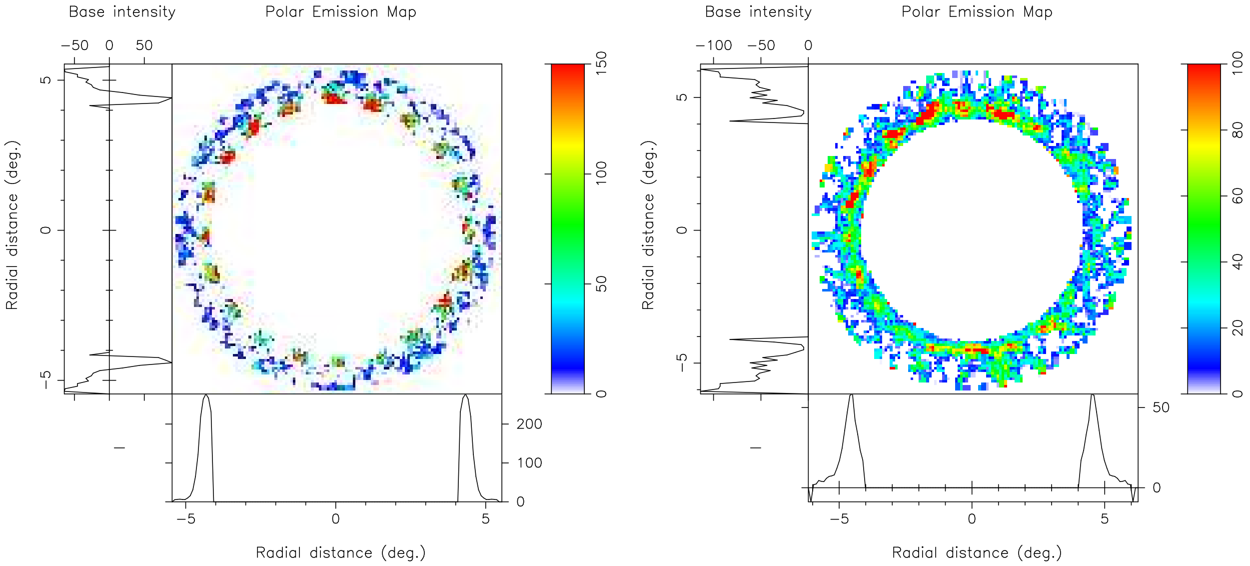

Figure 7. 'B'-mode polar maps on 27/12/90 at 103 (*left*) and 40 MHz (*right*) as in Fig. 5. This 103-MHz map is a good example of those in which the subbeams assume an antisymmetric distribution about the magnetic axis.

very brightest in both maps. Here, finally, we see what may be an actual correspondence between the patterns at the two frequencies—and at the same orientation.

V. THE 103/40-MHZ 'Q'-MODE BEAM STRUCTURE

The one fully 'Q'-mode observation in Table I (28/12) requires little discussion. As is not unexpected, both the 103- and 40-MHz recordings are quite weak; nonetheless, they represent some of the best such sequences in the Pushchino archive and were consequently chosen to provide a basis for the 'Q'-mode analysis and discussion in Suleymanova *et al* (1998). Polar maps of these data were constructed (not reproduced here), using a nominal value of the circulation time (36.5 P_1), and they exhibit no discernible correspondence whatsoever. The top of the 103-map shows two weak inner edge features at about '10:45' and '1 o'clock', while its 40-MHz pair exhibits emission centres at larger radii (or heights)—the brightest squarely at 'noon'. So, these two maps seem to differ in every possible manner: the patterns are wholly different at the two frequencies, and no rotation would help them to coincide. Moreover, the emission at both frequencies appears to come from somewhat different radii; that at 103 MHz shows a sharp inner-edge boundary as if cut off by the sightline traverse (just as we usually see at 430 MHz), while the 40-MHz pattern has a broader radial profile, though peaking at about the same value of some 4.7° [*cf.* the bottom panels of Figs. 5–7 (*right*)]. In short, our maps of this 'Q'-mode sequence seem utterly chaotic. It is important to remember that our 36.5-P_1 circulation-time value is only an estimate, though the PS is so short that this is not very critical.

The beginning of the first observation on 7/12 gives us the opportunity to examine the very end of a 'Q'-mode sequence, when perhaps the emission elements needed for the 'B-mode sequence are being reestablished. Then, we can estimate the circulation time using the short 'B'-mode sequence beyond it, which we noted above was about 36.5 P_1—and even if this is in error, we have a sequence of only about four times this length to map. It is worth mentioning that we see no hint of the primary modulation feature in these 'Q'-mode sequences, which is perhaps their primary defining feature.

The respective 103- and 40-MHz maps for these 'Q'-mode sequences in Figure 8 appear to show more correspondence than any we have examined thus far—though the S/N is poor owing to the weakness and shortness of the sequence, so careful inspection is required. In both, we find a strip of emission on the bottom inner edge of the pattern—and especially between about '4:30' and '8:30 o'clock'—which appears to continue around to '12' or '1' o'clock'. In both, the weakest and least orderly part of the pattern is between about '1:30' and '4:30'. Some features in the middle and outer parts of the patterns may also correspond; note particularly the bright outer-edge feature at about '4:30'. However, the inner-edge regions between about '4:30' and '8:30' are especially interesting; the higher frequency map indeed shows what appears to be a fairly regular series of some eight weak 'beamlets' over this 120° section of the map, and while the resolution of the 40-MHz map is poorer, a number of comparable features are seen here around its radial maximum.

Though we can only speculate about the significance of these weak and noisy patterns (weakness again being one of the usual characteristics of the 'Q' mode), these maps represent our first opportunity to examine a 'Q'-mode sequence which immediately precedes a transition to the 'B' mode. Here, indeed, we are examining the final 128 such pulses,

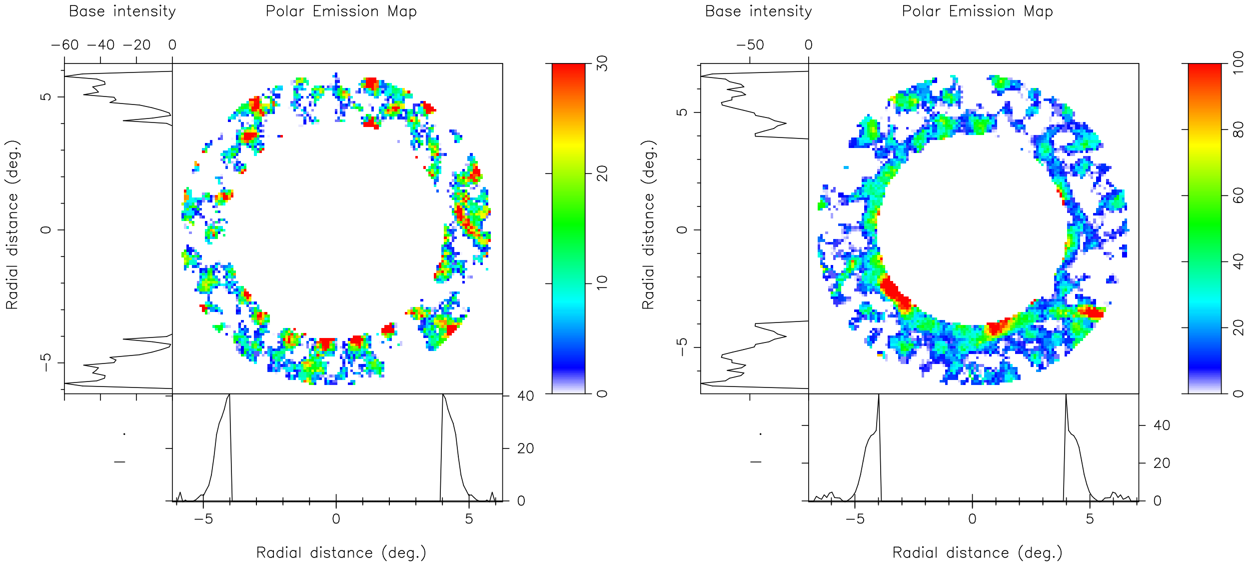

Figure 8. 'Q'-mode polar maps on 07/12/90 at 103 (*left*) and 40 MHz (*right*). These polar maps (as in Fig. 5) correspond to the last 128 pulses before the onset of the 'B' mode. They have been smoothed by a circular function 0.06° in diameter to improve the S/N.

prior to the abrupt 'B'-mode onset at pulse 281/312. Does the '4:30' feature represent one of the last 'Q'-mode subbeams, emitting here characteristically at a larger radius or height? And does the system of weak, inner edge 'beamlets' represent the reformation of the vigesimal 'B'-mode configuration? Note that these are too narrowly spaced, 8 in 120° or 24 overall, to generate the usual 'B'-mode modulation. Indeed, one can imagine that there are a total of about 20 such 'beamlets' around the inner edge of the pattern at 103 MHz, but, apart from the '4:30-to-8:30' group, they lie at discernibly irregular intervals. (It is also worth noting that 'B'-mode maps, constructed from the first 100 or so pulses following the transition, bear no resemblance to the 'last' 'Q'-mode maps we are examining here.)

Lastly, note that the emission in both 'Q'-mode patterns is on their leading edges. We see radial profiles which are truncated at the sightline impact angle β, not peaking well outside it as in all the other 'B'-mode maps encountered earlier. However seriously we take the above interpretation of the maps in Fig. 8, it does not begin to fully elucidate what electrodynamic conditions change so abruptly to reestablish the 'B'-mode patterns. In the space of one stellar rotation, not only does the strict, 20-fold subbeam pattern reassert itself, but the gross distribution of emission changes from one which is roughly symmetrical about the longitude origin (that of the magnetic axis) to one asymmetrically favoring earlier longitudes. Of course, we can readily note this abrupt change both in the raw sequences as well as in the different forms of the 'B'- and 'Q'-mode profiles—though we also now know from Suleymanova *et al* (1998) that slow variations precede 'B'-to-'Q'-mode changes. We will see below a variety of 'B'-mode polarisation characteristics.

VI. POLARISATION-MODE BEHAVIOUR

Linear polarisation information was available for all of the sequences, following the Faraday-modulation technique described above. On this basis it was possible to study the average profile polarisation and PA traverse as had been done earlier by Suleymanova *et al* (1998). The quality of the various observations was quite uneven—though in all cases it was possible to measure or estimate the mean fractional linear polarization to better than about 5%. These latter values are given in the right-most column of Table I, and the 103-MHz and Q-mode entries are shown in boldface and italics, respectively, to make comparison easier. The four highest quality 'B'-mode sequences, those on 23/12/90, 27/12/90, 13/02/91 and 23/01/92, are nearly equal in overall S/N, but vary markedly in average linear polarisation: the first two have only 20–25% linear polarisation, while the last two have some 40 and about 70%, respectively. The remaining 103-MHz 'B'-mode PSs all fall within this range, whereas the 103-MHz 'Q'-mode profiles consistently exhibit depolarised profiles with fractional linear less than 25%. Finally, the 40-MHz profiles polarization estimates suggest that the fractional linear variations correlate well with the higher frequency; we computed a correlation coefficient of some 60%.

Overall, a much larger proportion of the total samples at the higher frequency were strong enough to give a reliable estimate of the linear Stokes parameters Q and U, and only for one of these—the 103-MHz sequence on 23/12/90—was a significant proportion of secondary polarisation mode (SPM) samples detected. Among the four best 'B'-mode PSs mentioned above, the fractional linear variations are anticorrelated with the number of SPM-dominated samples detected. In PA histograms we see clear "patches" of SPM emission in the first two least linearly polarised PSs, less in

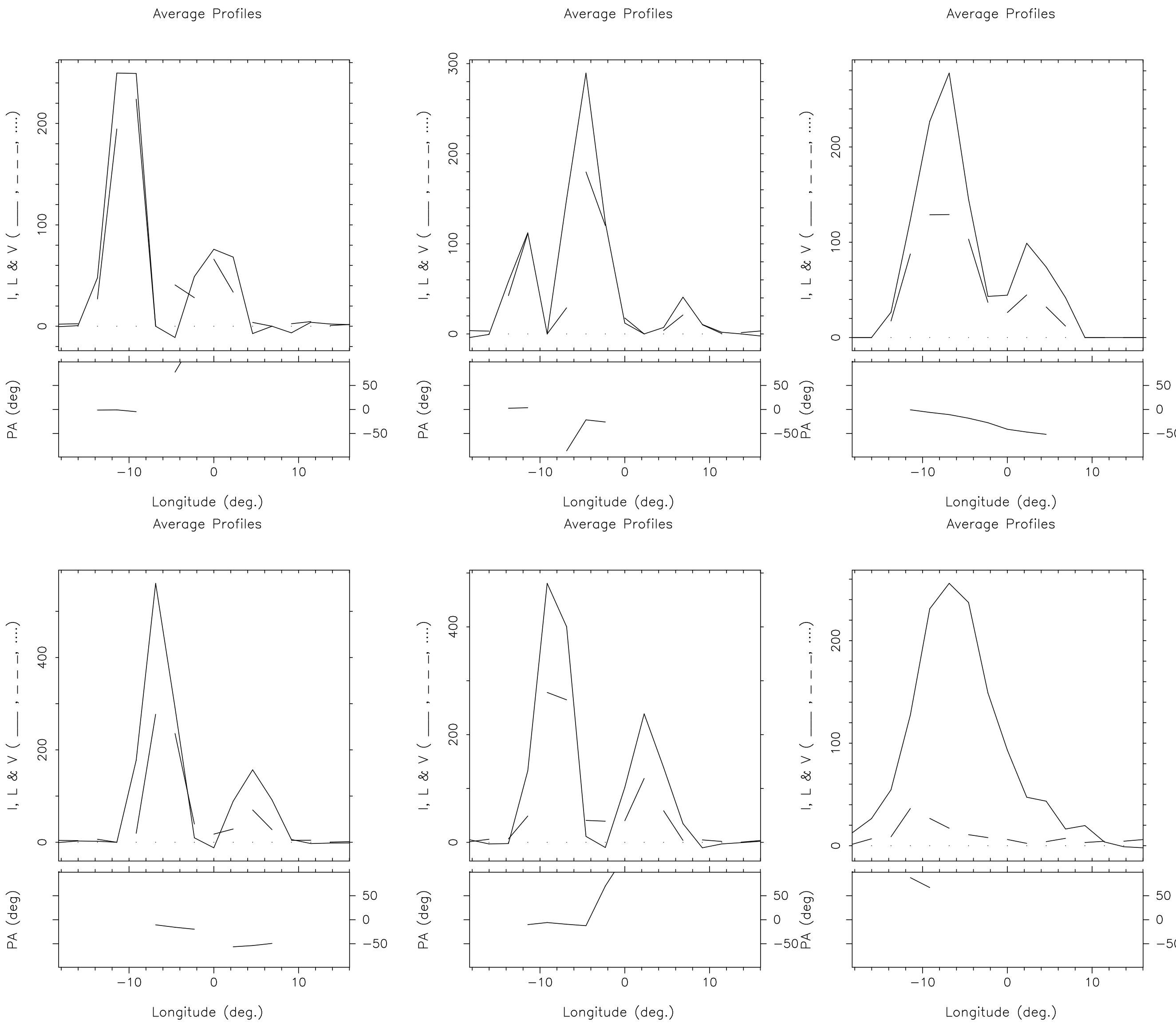

Figure 9. Composite of 4 partial polarisation profiles (*left, center*) folded at different phases of the nominal 1.87-P_1 modulation cycle as well as partial profiles of both the 'drifting' power (*top right*) and the 'base' (*bottom right*). All were computed from pulses 91–346 of the 27/12/90 'B'-mode sequence mapped in Fig. 7 (*left*). Two and at times three subpulses are seen in the four panels which 'drift' progressively from later to earlier phases about 3° from plot to plot. Note that their form and amplitude are windowed strongly by the overall double form of the average profile [not shown, but similar to that in the left-hand panel of Fig. 1 (*left*)]. Stokes V does not exist for these sequences, and thus the dotted curves are uniformly zero.

the 1991 PS, and no clear SPM emission at all in the last, most highly polarised observation.

It happened that most of the SPM samples in the 23/12/90 PS represented negative values of Stokes Q (such that little power was in Stokes U), so a polar map in this quantity (not shown) was computed and inspected. While it suggested a modal subbeam configuration much like that of the 430-MHz map in Paper I (fig. 19), unfortunately here also the SPM-dominated samples did not carry a very large fraction of the fluctuating power, so they were not easy to distinguish from the noise power in the map.

In a further effort to understand the modal character and variations of profile polarization, we computed sets of partial profiles corresponding to progressive quarter phases of the 1.87-P_1 modulation cycle—just as we did earlier in Paper I, fig. 6, for the 430-MHz observation. An example for 27/12/90 is given in the six panels of Figure 9, but similar analyses were carried out for the other three best 'B'-mode sequences above. The four left-most panels give the partial profiles at 90° modulation-phase intervals, and the 'drift' can be seen as a cyclical motion of the (mean) subpulses from right to left, some 3° longitude from panel to panel. The top- and bottom-right panels then show the forms of the mean 'drifter' and 'base,' respectively. Overall, the displays depict the behaviour of the PPM, as can be seen clearly in the 'drifter', although the slight residual polarisation of the 'base' is nearly orthogonal. Note, however, that the (mean) subpulses are highly polarised apart from some of their edges, where the depolarisation can be seen clearly. Here, indirectly, we are probably seeing the effects of the SPM, and some abrupt rotations of the PA (*cf.*panel b) further suggest near SPM dominance at these points.

Despite these detailed analyses, it is not entirely clear just what changes to produce the very great variations in 'B'-mode aggregate linear polarisation. The origin of the non-drifting 'base' emission is key to this understanding as it is necessarily defined by its total intensity but can accumulate as a result of the depolarisation. Overall, the subpulse polarization is very high, often appearing to reach 100%. SPM-associated depolarisation is very clear in the first two sequences, discernible in the third, but not so in the last observation. It would thus appear that changes in the modal configuration of the rotating subbeam system are required to produce the observed variations in the fractional linear polarisation—indeed, that the ratio of PPM to SPM power changes, but also that its angular offsets (and thus consequent depolarization characteristics) vary somewhat. Future observations with both better resolution and S/N will be needed to untangle these complicated effects.

VII. SUMMARY AND DISCUSSION

Above, we have studied observations of pulsar 0943+10, using mostly simultaneous 103- and 40-MHz sequences from the Pushchino Observatory. Eight of the observations were 'B'-mode sequences, three were 'Q'mode observations, and a further recorded a 'Q'-to-'B'-mode transition.

Our main results can be summarized as follows:

• The measured P_3 and $\hat{P}_3$ values for the five 'normal' 'B'-mode sequences fall within a narrow range just over 0.54 c/P_1 and around 37.7 P_1, respectively. Four other 'B'-mode sequences, one immediately following a 'Q'-mode sequence and another with an unusual symmetrical ('Q'-mode-like) 103-MHz profile, have P_3s well over 0.54 c/P_1 and $\hat{P}_3$ values around 36.5 P_1. Perhaps, these latter circulation times pertain more to what occurs during 'Q'-mode sequences.

• Of these 9 'B'-mode PSs, the 'normal' ones all have a weakish second component, while all of the 'Q'-mode-like ones show an accentuated (or more symmetrical) second component.

• In most cases the 103- and 40-MHz PS pairs exhibit small differences in circulation time $\hat{P}_3$. These differences represent only a few standard deviations in the errors, and such discrepancies could arise from random causes (*i.e.*, small differences in mean subbeam spacing). However, the behaviour appears orderly and suggests a slightly slower relative 40-MHz rotation for the 'normal' 'B'-mode sequences and a faster rotation of the 'Q'-mode-like ones.

• Maps of the Pushchino 103-MHz 'B'-mode sequences do not look very different than the Arecibo 111-MHz recording we analysed in Paper I (their fig. 26). However, six such sequences were here available for study. All exhibited the characteristic 20-fold subbeam pattern [see Figs. 5–7 (*left*)]. In some all 20 subbeams had comparable intensities, while in others, one or two subbeams were exceptionally bright. Finally, one had what appears to be a partially developed antisymmetric pattern with most of the emission on one 'side' of the pattern.

• Similarly, many of the Pushchino 40-MHz 'B'-mode sequences, look very much like the 35-MHz maps of the Gauribidanur observations in Paper II. However, here we can see that even as uniform a pattern as that of their G observation (Paper II, fig. 7) is quite unusual. Most of our observations result in maps more like the C series in Paper II (their fig. 6), with however perhaps even more corrugation of the subbeam intensity.

• We cannot know whether any correspondence between the systems of subbeam intensities at two frequencies would occur without a rotation between the patterns, so we have been open to this possibility. Generally, we have found very little discernible correspondence between the 103- and 40-MHz 'B'-mode maps pairs; indeed, for 5 of the 6 patterns, almost none. The single 'B'-mode observation which exhibits an apparent correspondence is the 27/12 sequence depicted in Fig. 7, and, if actual, the maps correspond without any relative rotation.

• Surprisingly, it is a pair of short 'Q'-mode maps which may show the most correspondence. The 7/12 sequence, which represents the first recording of a 'Q'-mode to 'B'-mode transition, exhibits corresponding bright and dim regions (without added rotation), particularly near the 'bottom', inner edge of the patterns. The 128-pulse sequence in question may indicate a series of up to 20 'beamlets', which are not uniformly spaced in azimuth, within the pattern. Eight of these around the bright bottom edge have regular spacings a little less than the usual 18° 'B'-mode configuration. It is interesting that the 'B'-mode sequence which commences immediately afterward has a pattern with little or nothing in common with this 'Q'-mode pattern.

• We confirm the earlier result that 'B'-mode profiles tend to be more highly polarised than their 'Q'-mode counterparts and that this results from differing ratios of PPM and SPM power. However, we have found a good deal of variation in the fractional linear polarisation of the profiles overall, and these variations appear well correlated between the two frequencies—again providing strong evidence that these are also produced by varying proportions of modal power.

• The 12 observations reported here were chosen from among a program of 22 1990-December sequences for their good quality at both 103 and 40 MHz. Therefore, the relative occurrance frequency of 'B'-mode and 'Q'-mode sequences has been skewed. The ratio first reported by Suleymanova & Izvekova (1984)—about equal—was confirmed using the full set by Suleymanova *et al* (1998).

• These PRAO observations, together with those considered in Papers I & II comprise some 8000 pulses, during which two modal transitions were encountered—one of each type. If 'B'- and 'Q'-mode sequences represent a cycle, then we might estimate that its duration is some 2.5 hours or so and that 'B'-mode sequences persist for 1.5 hours or some 5000 pulses. It will be interesting, when longer sequences become available, to see how these estimates bear on their reality.

These Pushchino observations give further credence to the picture that subpulse emission takes place in connection with a series of emission columns, which, being 'seeded' in the polar cap region near the surface of the star, rise up through the polar flux tube into the emission zone at a height of several hundred kilometers, and then extend out to much greater distances, perhaps into the ambient medium around the star. Pulsar 0943+10's rotation axis makes only a small angle with its magnetic-polar axis, so these emission columns would extend in a direction nearly parallel to the rotation axis (or along the centre of the velocity-of-light cylinder). The stable 'B'-mode system is configured of just 20 such columns, whose integrity we have seen maintained throughout the range of emission heights sampled by our various observations. We do see, however, a progressive disordering of the subbeam configuration—little between 430 and 111 MHz, but perceptibly more at 35 and 40 MHz. Using the model of Paper I (see Table 2), the former lie within about 15 km or each other at 131 and 147 km; whereas, the latter are some 30 km further away at some 170 km‖.

During the 'B'-mode sequences, we might speculate that this system of emission columns undergoes a progressive twisting by the rotating star (recall that its rotation and magnetic axes are closely aligned)—most of it presumably well above the emission regions where the magnetic field weakens sufficiently. We might then expect that there is some physical maximum to the amount of distortion this system of emission columns can sustain, and, that exceeding this maximum produces an unstable, much simpler emission beam configuration which we know as that of the 'Q' mode. During these sequences emission may be excited along some of these same columns, but in the dramatic, but disorganized manner characteristic of the 'Q' mode. Then, after some time, when the emission-column distortion has had a chance to recover, another stable 'B'-mode configuration can be reinstituted.

While features of this overall picture may describe the physical conditions producing 0943+10's modal sequences, including both the near instantaneous 'snap' transitions at the modal boundaries as well as the slow changes in intensity and profile form which were identified by Suleymanova *et al* (1998), other aspects of the modal changes remain unclear. To wit, the 'B'-mode emission distribution is characteristically asymmetric about the longitude of the magnetic axis—or, what is the same, their profiles usually show most of the power at negative longitudes—whereas, 'Q'-mode power is either roughly symmetric or even favoring of trailing longitudes. Given our now clear understanding that the subbeam rotation is continuous—and thereby symmetrical about the magnetic axis—these asymmetries, along with their both slow and rapid variations, assume a new significance.

‖ The outer-cone-model heights for 430, 111/103, and 35/40 MHz are 231, 261 and 300-km, respectively. See Mitra & Rankin (2002) for more physical height values corresponding to these model computations.

Physically, the remarkable coherence of this pulsar's subbeam patterns over the entire frequency range that pulse-sequence observations are possible—nearly 4 octaves—points strongly to an $\mathbf{E}\times\mathbf{B}$ drift mechanism as first suggested by Ruderman & Sutherland (1975). Whether, however, this model's other physical expectations (including that the primary particle acceleration occurs just above the magnetic polar cap) remains an open, but now actively debated question [*e.g.* Asseo & Khechinashvili (2002); Gil, Melichidze & Mitra (2002); Wright (2002)].

This all said, we see that pulsar B0943+10, having been the agency of considerable new knowledge about its conditions of emission, still has a great deal to teach us. Studies of long sequences—which continuously encounter a few mode changes—should provide answers to some of the questions above. New and better polarimetry will also provide new insights as will study of other pulsars with both similar and dissimilar properties.

Acknowledgements: It is a pleasure to thank both Slava Pugachev for assistance in developing programs used in the observations and analysis, and Geoff Wright for his critical comments on the paper in draft. One of us (JMR) also wishes acknowledge the hospitality of the Raman Research Institute where this work was initiated. This work was also supported in part by US NSF grants AST 99-86754 and 00-98685 as well as under a visitor grant from the Nederlandse Organisatie voor Wetenschappelijk Onderzoek.

References

Asseo E., & Khechinashvili, D. 2002, M.N.R.A.S., 334, 743.
Asgekar A. A., & Deshpande, A. A. 2001, M.N.R.A.S., 326, 1249.
Backer, D. C., Rankin, J. M., & Campbell, D. C. 1975, Ap.J., 197, 481.
Deshpande A. A., 1999, *IAU Colloquium #177* Bonn, 149
Deshpande A. A., Rankin J. M., 1999, Ap.J., 524, 1008
Deshpande A. A., Rankin J. M., 2001, M.N.R.A.S., 322, 438
Ferraro V. C. A., Plumpton C., 1966, *Magneto-Fluid Mechanics* (London: Oxford University Press), 23
Gil, J. A., Melichidze, G. I., & Mitra, D. 2002, A&A, 388, 246.
Mitra, D., & Rankin, J. M. 2002, Ap.J., 577, 322 (2002).
Rankin J. M., Deshpande A. A., 1999, *IAU Colloquium #177* Bonn, 155
Ruderman M. A., Sutherland P. G., 1975, Ap.J., 196, 51
Suleymanova S. A., Izvekova V. A., 1984, Sov. Astron. 28, 53
Suleymanova S. A., Izvekova V. A, Rankin J. M., Rathnasree N., 1998, JAA, 19, 1
Suleymanova, S. A., Volodin, Yu. V. & Shitov, Yu. P. 1988, Astron.Zh. 65, 349.
Wright, G. A. E. 2002, M.N.R.A.S., in press.